Interactions of the 8-kDa Domain of Rat DNA Polymerase β with DNA†

Maria J. Jezewska, Surendran Rajendran, and Wlodzimierz Bujalowski*

Department of Human Biological Chemistry and Genetics, Sealy Center for Structural Biology, The University of Texas Medical Branch at Galveston, 301 University Boulevard, Galveston, Texas 77555-1053

Received December 1, 2000; Revised Manuscript Received January 18, 2001

ABSTRACT: Interactions between the isolated 8-kDa domain of the rat DNA polymerase β and DNA have been studied, using the quantitative fluorescence titration technique. The obtained results show that the number of nucleotide residues occluded in the native 8-kDa domain complex with the ssDNA (the site size) is strongly affected by Mg^{2+} cations. In the absence of Mg^{2+}, the domain occludes 13 ± 0.7 nucleotide residues, while in the presence of Mg^{2+} the site size decreases to 9 ± 0.6 nucleotides. The high affinity of the magnesium cation binding, as well as the dramatic changes in the monovalent salt effect on the protein−ssDNA interactions in the presence of Mg^{2+}, indicates that the site size decrease results from the Mg^{2+} binding to the domain. The site size of the isolated domain−ssDNA complex is significantly larger than the 5 ± 2 site size determined for the (pol β)$_5$ binding mode formed by an intact polymerase, indicating that the intact enzyme, but not the isolated domain, has the ability to use only part of the domain DNA-binding site in its interactions with the nucleic acid. Salt effect on the intrinsic interactions of the domain with the ssDNA indicates that a net release of $m \approx 5$ ions accompanies the complex formation. Independence of the number of ions released upon the type of anion in solution strongly suggests that the domain forms as many as seven ionic contacts with the ssDNA. Experiments with different ssDNA oligomers show that the affinity decreases gradually with the decreasing number of nucleotide residues in the oligomer. The data indicate a continuous, energetically homogeneous structure of the DNA-binding site of the domain, with crucial, nonspecific contacts between the protein and the DNA evenly distributed over the entire binding site. The DNA-binding site shows little base specificity. Moreover, the domain has an intrinsic affinity and site size of its complex with the dsDNA conformation, similar to the affinity and site size with the ssDNA. The significance of these results for the mechanistic role of the 8-kDa domain in the functioning of rat pol β is discussed.

Polymerase β (pol β) plays a very specialized function in the DNA repair machinery in mammalian cells (*1*−*7*). Pol β conducts "gap-filling" synthesis on gapped DNA in a processive fashion (*2*, *4*−*6*, *8*, *9*). The in vitro gap-filling reaction has been proposed as being consistent with the role of pol β in the gap-filling synthesis involved in mismatch repair (*4*, *5*, *7*) and in the repair of monofunctional adducts, UV damaged DNA, and abasic lesions in DNA (*8*−*14*). These specific functions are reflected in the "simplified" activities of the pol β. The enzyme lacks accessory activities, such as 3′ or 5′ exonuclease, endonuclease, dNMP turnover, and pyrophosphorolysis (*2*, *4*−*7*).

Pol β is one of several recognized DNA-directed polymerases of the eukaryotic nucleus (*1*−*3*, *15*). Rat pol β is a single polypeptide of ∼39 kDa (*16*−*20*). Due to its resemblance to the human hand, the crystal structure of the enzyme revealed a typical polymerase fold consisting of a thumb, palm, and fingers (*18*, *19*). These structural elements form the large catalytic 31-kDa domain of the enzyme (*20*, *21*). However, a characteristic feature of the pol β structure is the presence of an extra, small 8-kDa domain that is connected with the tip of the fingers through a tether of 14 amino acids (*18*, *19*).

The domain structure of the pol β has been proposed to have a profound effect on enzyme interactions with the DNA. Solution studies showed that the 8-kDa domain has a high affinity for a single-stranded nucleic acid, leading to the suggestion that it is the template-binding domain, while the dsDNA[1] affinity resides in the 31-kDa catalytic domain (*20*, *21*). However, studies with the isolated 8-kDa domain clearly indicate that the domain also has dsDNA binding ability (*14*). Moreover, our recent analyses of rat and human pol β binding to the ssDNA have shown very complex patterns in enzyme interactions with the nucleic acid (*22*, *23*). The enzymes bind the ssDNA in two binding modes, differing in the number of occluded nucleotide residues (*22*, *23*). We designated the first complex as the (pol β)$_{16}$ and the second as the (pol β)$_5$ binding mode. In the (pol β)$_{16}$ binding mode, not only the small 8-kDa domain but also the large 31-kDa catalytic domain of the enzyme is involved in interactions with the ssDNA. In the (pol β)$_5$ binding mode, the small 8-kDa domain is predominantly engaged in interactions with the ssDNA (*22*, *23*). Moreover, the binding modes differ in their

† This work was supported by NIH Grant GM-58565 (to W.B.).

* To whom correspondence should be addressed. Tel: (409) 772-5634. Fax: (409) 772-1790. E-mail: wbujalow@utmb.edu.

[1] Abbreviations: ssDNA, single-stranded DNA; dsDNA, double-stranded DNA; MCT method, macromolecular competition titration method; HhH, helix−hairpin−helix.

10.1021/bi002749s CCC: $20.00
Published on Web 02/17/2001

affinities and abilities to induce conformational changes in the ssDNA (*22*, *23*).

Preliminary studies with the isolated 8-kDa domain indicate that the site size of the domain−ssDNA complex is significantly larger than the site size of the (pol β)$_5$ binding mode (*22*). The lack of significant cooperative interactions between protein molecules bound in the (pol β)$_5$ binding mode indicates that interactions between the domain and the nucleic acid are the major source of the free energy of binding in this mode, despite the limited access of the domain to the ssDNA, as compared to the isolated domain *(22*).

Elucidation of 8-kDa domain interactions with the DNA is of paramount importance for our understanding the role of the domain in the functioning of pol β. In this paper, we report the quantitative analyses of the interactions of the native, isolated 8-kDa domain of rat pol β with both ssDNA and dsDNA. We provide direct evidence that the site size of the 8-kDa domain−ssDNA complex depends on the presence of Mg^{2+} cations. The magnesium effect results from binding the Mg^{2+} cations to the domain. The much larger site size of the domain−ssDNA complex than the site size of the (pol β)$_5$ binding mode indicates that the intact enzyme has the ability to use only a part of the domain DNA-binding site, when interacting with the ssDNA. The obtained data indicate the DNA-binding site has a continuous, energetically homogeneous structure with a large number of similar, nonspecific contacts between the protein and the DNA. Moreover, the binding site shows little base specificity and has significant intrinsic affinity for the dsDNA conformation.

MATERIALS AND METHODS

Reagents and Buffers. All chemicals were reagent grade. All solutions were made with distilled and deionized >18 MΩ (Milli-Q Plus) water. Buffer C is 10 mM sodium cacodylate adjusted to pH 7.0 with HCl, 1 mM $MgCl_2$, and 10% glycerol. Buffer C1 is the same as buffer C but without $MgCl_2$. The temperatures and concentrations of NaCl in the buffer are indicated in the text.

Recombinant, Native Rat Pol β 8-kDa Domain. The plasmid harboring the gene of the 8-kDa domain of rat pol β was a generous gift from Dr. S. H. Wilson (NIEHS). However, sequencing the gene revealed that the amino acid residue in location 87, at the C-terminus of the protein, is aparagine, not lysine, as indicated by the primary structure of the entire enzyme molecule (*16*). We replaced the asparagine residue with the original lysine. Moreover, the gene of the protein has been placed in plasmid pET30a, under control of the T7 polymerase system. Isolation and purification of the protein were performed as previously described (*16*, *20*, *22*−*24*). The concentration of the protein was spectrophotometrically determined using the extinction coefficient $\epsilon_{280} = 4.45 \times 10^3$ cm^{-1} M^{-1}, obtained with the approach based on Edelhoch's method (*22*, *23*, *25*−*29*).

Nucleic Acids. All nucleic acids were purchased from Midland Certified Reagents (Midland, TX). The etheno derivatives of the nucleic acids were obtained by modification with chloroacetaldehyde (*22*, *23*, *27*, *28*, *30*−*32*). This modification goes to completion and provides a fluorescent derivative of a nucleic acid. The concentrations of poly(dϵA), poly(dA), poly(dT), and poly(dC) were spectrophotometrically determined using extinction coefficients $\epsilon_{257} = 3700$, $\epsilon_{260} = 10000$, $\epsilon_{260} = 8100$, and $\epsilon_{270} = 7200$ M^{-1} cm^{-1} (nucleotide) (*23*). The concentrations of the ssDNA oligomers were determined using the nearest-neighbor analysis, as previously described (*22*, *23*). The dsDNA was formed by mixing an equal amount of both strands, warming the mixture to 95 °C for 5 min, and cooling slowly to room temperature, over a period of 3−4 h (*22*, *23*).

Fluorescence Measurements. All steady-state fluorescence titrations were performed using the SLM-AMINCO 8100 and 48000S spectrofluorometers. To avoid possible artifacts, due to the fluorescence anisotropy of the sample, polarizers were placed in excitation and emission channels and set at 90° and 55° (magic angle), respectively. The binding was followed by monitoring the fluorescence of the etheno derivatives ($\lambda_{ex} = 325$ nm, $\lambda_{em} = 410$ nm). Computer fits were performed using Mathematica (Wolfram, IL) and KaleidaGraph (Synergy Software, PA). The nucleic acid relative fluorescence increase, ΔF, upon binding the 8-kDa domain is defined as $\Delta F = (F_i - F_0)/F$, where F_i is the fluorescence of the nucleic acid at a given titration point "*i*", and F_0 is the initial value of the fluorescence of the nucleic acid sample (*26*−*28*).

Quantitative Determination of Stoichiometries and Binding Isotherms of the Rat Pol β 8-kDa Domain−ssDNA Complexes. In this work, we followed the binding of the rat pol β 8-kDa domain to the ssDNAs by monitoring the fluorescence increase, ΔF, of the nucleic acid etheno derivatives upon the complex formation. The method of obtaining rigorous estimates of the average binding density, $\sum \nu_i$ (number of domain molecules bound per nucleotide), and the free protein concentration, P_F, has been previously described in detail by us (*32*−*36*). Briefly, the experimentally observed ΔF has a contribution from each of the different possible *i* complexes of the 8-kDa domain with the ssDNA. Thus, the observed fluorescence increase is functionally related to $\sum \nu_i$ by

$$\Delta F = \sum \nu_i \Delta F_{i_{max}} \tag{1}$$

where $\Delta F_{i_{max}}$ is the molecular parameter characterizing the maximum fluorescence increase of the nucleic acid with the 8-kDa domain bound in complex *i*. The same value of ΔF, obtained at two different total nucleic acid concentrations, N_{T_1} and N_{T_2}, indicates the same physical state of the nucleic acid, i.e., the degree of binding, $\sum \nu_i$, and the free domain concentration, P_F, must be the same. The values of $\sum \nu_i$ and P_F are then related to the total protein concentrations, P_{T_1} and P_{T_2}, and the total nucleic acid concentrations, N_{T_1} and N_{T_2}, at the same value of ΔF, by

$$\sum \nu_i = \frac{P_{T_2} - P_{T_1}}{N_{T_2} - N_{T_1}} \tag{2a}$$

$$P_F = P_{T_x} - (\sum \nu_i) N_{T_x} \tag{2b}$$

where $x = 1$ or 2 (*32*−*36*).

Analysis of the Binding Isotherms of the 8-kDa Domain−Poly(dεA) System. The simplest statistical thermodynamic model that describes the binding of a large ligand that occludes a number of *n* nucleotides in the complex (site size) to an infinite, homogeneous lattice is the McGhee−von

Hippel model (*37*). Once the site size, *n*, of the complex is known, this paradigm model allows one to extract an intrinsic binding constant *K* and a parameter ω, characterizing the cooperative interactions between bound ligand molecules, and takes into account the overlap among potential binding sites. Previously, we derived a single, generalized equation for the McGhee−von Hippel model that can be applied to both cooperative and noncooperative binding (*38*). The binding density, $\sum\nu_i$, is described by the generalized equation as

$$\sum\nu_i = K(1-n\sum\nu_i)\left\{\frac{2\omega(1-n\sum\nu_i)}{(2\omega-1)(1-n\sum\nu_i)+\sum\nu_i+R}\right\}^{n-1}\times \left\{\frac{1-(n+1)\sum\nu_i+R}{2(1-n\sum\nu_i)}\right\}^2 P_F \quad (3)$$

where $R = \{[1-(n+1)\sum\nu_i]^2 + 4\omega\sum\nu_i(1-n\sum\nu_i)\}^{0.5}$ (*38*).

Quantitative Determination of Binding Isotherms of Rat Pol β 8-kDa Domain Interactions with Unmodified, ssDNA Homopolymers. Application of the MCT Method. Determination of the interaction parameters for the rat pol β 8-kDa domain−unmodified nucleic acid complexes has been performed using the macromolecular competition titration (MCT) method (*27*). In this method, the fluorescent reference nucleic acid [e.g., poly(dϵA)] at total concentration, N_{T_R}, is titrated with the protein in the presence of a competing nonfluorescent nucleic acid [e.g., poly(dT)] of the total concentration, N_{T_S}. The total concentration of the protein, P_T, at which the same value of the relative fluorescence increase, ΔF, of the reference nucleic acid is observed in the absence of the unmodified ssDNA, P_{T_R}, and in the presence of the unmodified ssDNA, P_{T_S}, is defined as (*27*)

$$P_{T_R} = (\sum\nu_i)_R N_{T_R} + P_F \quad (4a)$$

$$P_{T_S} = (\sum\nu_i)_R N_{T_R} + (\sum\nu_i)_S N_{T_S} + P_F \quad (4b)$$

where $(\sum\nu_i)_R$, $(\sum\nu_i)_S$, and P_F are the binding density of the 8-kDa domain on the reference nucleic acid, the binding density of the protein on the nonfluorescent, competing nucleic acid, and the free protein concentration, respectively. Solving eqs 4a and 4b for $(\sum\nu_i)_S$ and P_F provides the thermodynamically rigorous binding density of the 8-kDa domain on an unmodified ssDNA and the free protein concentration defined as (*27*)

$$(\sum\nu_i)_S = \frac{P_{T_S} - P_{T_R}}{N_{T_S}} \quad (5a)$$

and

$$P_F = P_{T_S} - (\sum\nu_i)_S N_{T_S} - (\sum\nu_i)_R N_{T_R} \quad (5b)$$

Analysis of the Lattice-Competition Binding Isotherms. Once the site size of the 8-kDa domain on the unmodified polymer DNA has been determined, fluorescence titration curves of the fluorescent, reference nucleic acid, in the presence of the unmodified ssDNA, can be analyzed using the approach previously described by us (*27*). Ligand binding to two competing nucleic acid lattices is described by two independent isotherms defined by eq 3. However, any attempt to simultaneously use two isotherms, of the type given by eq 3, is hindered by the fact that they are complex, polynomial, implicit functions of the binding density, $\sum\nu_i$, and free ligand concentration, $\sum\nu_i[F(\sum\nu_i,P_F)]$. Thus, to simulate, or fit, the competition titration isotherms of large ligand binding to two competing nucleic acid lattices, complex and cumbersome numerical calculations are required (*27*). The general approach that overcomes this problem is based on the combined application of the generalized McGhee−von Hippel equation, as defined by eq 3, and the exact combinatorial theory for large ligand binding to a linear, homogeneous lattice (*27*, *38*, *39*). In the combinatorial approach for the cooperative binding of a large ligand, which covers *n* nucleotide residues, the partition function of the ligand−lattice system, *Z*, is defined by

$$Z = \sum_{k=0}^{g}\sum_{j=0}^{k-1} P_M(k,j)(K_S P_F)^k \omega_S^{\,j} \quad (6a)$$

where *g* is the maximum number of ligand molecules which may bind to the finite nucleic acid lattice (for the nucleic acid lattice *M* residues long, $g = M/n$), K_S is the intrinsic binding constant for the binding to an unmodified, nucleic acid lattice, ω_S is the cooperative interaction parameter, *k* is the number of ligand molecules bound, and *j* is the number of cooperative contacts between the *k* bound ligand molecules in a particular configuration on the lattice. The combinatorial factor $P_M(k,j)$ is the number of distinct ways that *k* ligands bind to a lattice, with *j* cooperative contacts, and is defined by

$$P_M(k,j) = \frac{(M-nk+1)!(k-1)!}{(M-nk+j+1)!(k-j)!(k-j-1)!} \quad (6b)$$

The binding density, $(\sum\nu_i)_S$, is then obtained by using the standard statistical thermodynamic expression, $(\sum\nu_i)_S = \partial \ln Z/\partial \ln P_F$, as

$$(\sum\nu_i)_S = \frac{\sum_{k=1}^{g}\sum_{j=0}^{k-1} kP_M(k,j)(K_S P_F)^k \omega_S^{\,j}}{\sum_{k=0}^{g}\sum_{j=0}^{k-1} P_M(k,j)(K_S P_F)^k \omega_S^{\,j}} \quad (7)$$

Equations 6 and 7 describe the binding of a large ligand to a finite, linear homogeneous lattice. For a long enough lattice, the obtained isotherm will be, within experimental accuracy, indistinguishable from the isotherm generated using the generalized eq 3 for binding the large ligand to the infinite lattice. We found that in the case of a protein, like the 8-kDa domain ($n = 9-13$), a lattice which can accommodate >60 protein molecules (600 nucleotides) represents an "infinite" lattice for any practical purpose (*27*).

Contrary to the generalized McGhee−von Hippel eq 3, expression 7 is an explicit function of the free ligand concentration which allows us to directly calculate the binding density on the unmodified ssDNA for the known *K*, ω, *n*, and P_F. Notice, through eq 3 the free ligand concentration can be explicitly calculated using an infinite lattice

model. Thus, combining both models offers a simple and very efficient way of fitting the simultaneous binding of a large ligand to two (or more) competing, different linear lattices, e.g., a reference fluorescent nucleic acid in the presence of a competing, nonfluorescent nucleic acid (*27*). This is accomplished by first applying eq 3 to the reference fluorescent nucleic acid, calculating the free ligand concentration of P_F for given values of parameters K, ω, and n, with $(\sum\nu_i)_R$, as a variable. Subsequently, the obtained value of P_F is introduced into eq 7, which is used to describe the protein binding to a competing, nonfluorescent nucleic acid, and the binding density, $(\sum\nu_i)_S$, is calculated for the given K_S, ω_S, and n_S, which characterize the binding of the protein to the competing lattice. The calculations are repeated for the entire range of $(\sum\nu_i)_R$, generating the required $(\sum\nu_i)_S$ for the competing nucleic acid lattice, as a function of P_F. The experimental binding isotherm, which is the observed fluorescence change, ΔF, as a function of the total protein concentration, P_T, is then obtained by calculating the total protein concentration, P_T, for each value of ΔF, by introducing $(\sum\nu_i)_S$, $(\sum\nu_i)_R$, and P_F into eq 4b (*27*).

RESULTS

Stoichiometry of the Rat Pol β 8-kDa Domain−ssDNA Complexes in the Presence and Absence of Mg^{2+} Cations. Fluorescence titrations of poly(dϵA) with the rat pol β 8-kDa domain, at two different nucleic acid concentrations, in buffer C1 (pH 7.0, 10 °C), containing 50 mM NaCl, are shown in Figure 1a. The relative increase of the nucleic acid fluorescence reaches the value of $\Delta F_{max} = 1.3 \pm 0.1$. At higher nucleic acid concentrations, a given fluorescence increase is reached at higher enzyme concentrations, due to the extra nucleic acid in the solution. The selected nucleic acid concentrations provide a separation of the isotherms up to the relative fluorescence increase of $\Delta F \approx 0.9$, i.e., up to ~75% of the binding curve. Notice that the observed maximum fluorescence increase is significantly lower than $\Delta F_{max} = 2.1 \pm 0.1$, previously obtained with the 8-kDa domain with asparagine in location 87 instead of lysine (*22*). Such a large difference between the observed values of ΔF_{max} indicates that the structure of the ssDNA in the complex with the native domain is significantly different than in the case of the domain containing the mutation (see Discussion).

To obtain thermodynamic binding isotherms, independent of any assumption about the relationship between the observed signal and the binding density, $\sum\nu_i$, the titration curves in Figure 1a have been analyzed, using the approach outlined in Materials and Methods (*32*−*36*). Figure 1b shows the dependence of the observed relative fluorescence increase, ΔF, as a function of the average binding density, $\sum\nu_i$. The plot is linear and shows the existence of a single binding phase. Short extrapolation of the binding density to the maximum fluorescence increase at saturation provides $\sum\nu_i = 0.077 \pm 0.005$, which shows that, in the absence of Mg^{2+}, the isolated 8-kDa domain occludes $n = 13 \pm 0.7$ nucleotide residues in the complex with the ssDNA. Because we know the site size of the complex, and the domain binds to the ssDNA in a single phase with $\Delta F_{max} = 1.3 \pm 0.1$, we can use the generalized McGhee−von Hippel equation to extract the remaining two interaction parameters, the intrinsic binding constant, K, and the cooperativity parameter, ω (eq 3). The solid lines in Figure 1a are computer fits of the experimental isotherms, using eq 3. The theoretical lines provide an excellent fit to the experimental isotherms with $K = (1 \pm 0.3) \times 10^6$ M^{-1} and $\omega = 2.2 \pm 0.7$ (Table 1).

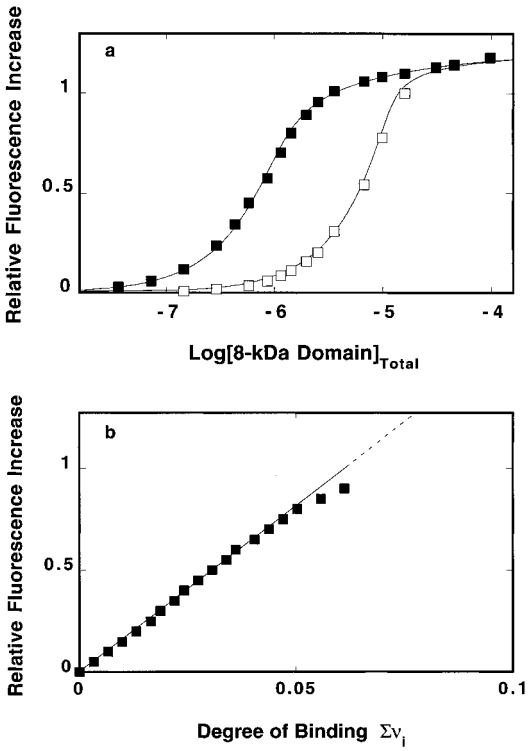

FIGURE 1: (a) Fluorescence titrations ($\lambda_{ex} = 325$ nm, $\lambda_{em} = 410$ nm) of poly(dϵA) with the 8-kDa domain of rat pol β in buffer C1 (pH 7.0, 10 °C), containing 50 mM NaCl, at two different concentrations of the nucleic acid (nucleotide): (■) 2×10^{-5} M; (□) 1.93×10^{-4} M. The solid lines are computer fits of the fluorescence isotherms using the generalized McGhee−von Hippel model, as defined by eq 3, using a single set of parameters: $K = 1 \times 10^6$ M^{-1}, $n = 13$, $\omega = 2.3$, and $\Delta F_{max} = 1.27$ (details in text). Errors in determining the parameters, provided in the text, are standard deviations obtained using four to five independent titration experiments. (b) Dependence of the relative fluorescence change, ΔF, upon the binding density, $\Sigma\nu_i$, of the 8-kDa domain on poly(dϵA) (■). The average binding density, $\Sigma\nu_i$, has been quantitatively determined using the method described in Materials and Methods (*27*). The solid, straight line follows the points and does not have a theoretical basis. The dashed line is an extrapolation of the binding density to the maximum value of the relative fluorescence change, $\Delta F_{max} = 1.27$, which provides $\Sigma\nu_i = 0.077 \pm 0.05$, corresponding to the site size of the domain−ssDNA complex, $n = 13 \pm 0.6$.

Table 1: Intrinsic Binding Constant, K, Cooperativity Parameter, ω, Site Size, n, and Maximum Fluorescence Increase, ΔF_{max}, for Rat Pol β 8-kDa Domain Binding to Poly(dϵA) in the Absence of $MgCl_2$ [Buffer C1 (pH 7.0, 10 °C) Containing 50 mM NaCl] and the Presence of 1 mM $MgCl_2$ [Buffer C (pH 7.0, 10 °C) Containing 50 mM NaCl][a]

$MgCl_2$	K (M^{-1})	ω	n	ΔF_{max}
0	$(1 \pm 0.3) \times 10^6$	2.2 ± 0.7	13 ± 0.7	1.3 ± 0.1
1 mM	$(2.8 \pm 0.5) \times 10^5$	1.5 ± 0.5	9 ± 0.6	1.4 ± 1

[a] Errors are standard deviations determined using three to four independent titration experiments.

Notice that the value of n is significantly larger than the site size, $n = 10 \pm 0.6$, previously obtained for the modified 8-kDa domain in the presence of 1 mM $MgCl_2$ (*22*). To address the effect of magnesium on the stoichiometry of the native rat pol β 8-kDa domain, we performed fluorescence titrations of poly(dϵA) with the domain at two different

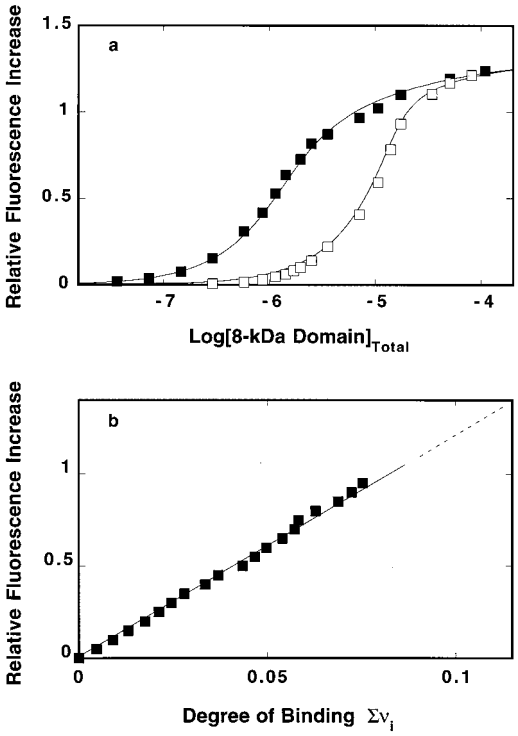

FIGURE 2: (a) Fluorescence titrations (λ_{ex} = 325 nm, λ_{em} = 410 nm) of poly(dϵA) with the 8-kDa domain of rat pol β in buffer C (pH 7.0, 10 °C), containing 50 mM NaCl, at two different concentrations of the nucleic acid (nucleotide): (■) 2×10^{-5} M; (□) 1.94×10^{-4} M. The solid lines are computer fits of the fluorescence isotherms using the generalized McGhee−von Hippel model, as defined by eq 3, using a single set of parameters: $K = 3 \times 10^5$ M^{-1}, $n = 9$, $\omega = 1.5$, and $\Delta F_{max} = 1.4$ (details in text). Errors in determining the parameters, provided in the text, are standard deviations obtained using four to five independent titration experiments. (b) Dependence of the relative fluorescence change, ΔF, upon the binding density, $\Sigma\nu_i$, of the 8-kDa domain on poly(dϵA) (■). The average binding density, $\Sigma\nu_i$, has been quantitatively determined using the method described in Materials and Methods (*27*, *34*). The solid straight line follows the points and does not have a theoretical basis. The dashed line is an extrapolation of the binding density to the maximum value of the relative fluorescence change, $\Delta F_{max} = 1.4$, which provides $\Sigma\nu_i = 0.115 \pm 0.005$, corresponding to the site size of the domain−ssDNA complex, $n = 9 \pm 0.6$.

nucleic acid concentrations, in buffer C (pH 7.0, 10 °C), containing 50 mM NaCl. The titration curves are shown in Figure 2a. In the presence of magnesium, the relative increase of the nucleic acid fluorescence reaches the value of $\Delta F_{max} = 1.4 \pm 0.1$, which is still significantly lower than the $\Delta F_{max} = 2.1 \pm 0.1$ previously obtained with the modified 8-kDa domain (*22*). Figure 2b shows the dependence of the observed relative fluorescence increase, ΔF, as a function of the average binding density, $\sum\nu_i$. In the presence of Mg^{2+}, the plot is also linear and shows the existence of a single binding phase. However, short extrapolation of the binding density to the maximum fluorescence increase at saturation provides $\sum\nu_i = 0.115 \pm 0.005$, which shows that in the presence of magnesium the native 8-kDa domain occludes 9 ± 0.6 nucleotide residues in the complex with the ssDNA. Thus, in the presence of Mg^{2+}, binding of the native 8-kDa domain to the ssDNA is characterized by different fluorescence changes and the site size of the complex than observed for the modified domain (*22*).

It is evident that the presence of 1 mM $MgCl_2$ has a dramatic effect on the stoichiometry of the 8-kDa domain−ssDNA complex. A further magnesium concentration increase does not lead to a further decrease of the site size of the complex. We also performed experiments with a modified 8-kDa domain, in the absence of magnesium, and observed a similar increase of the number of occluded nucleotide residues by the protein (data not shown). These results indicate that the presence of the single mutation in the modified 8-kDa domain does not eliminate the magnesium effect on the observed stoichiometry of the complex. The solid lines in Figure 2a are computer fits of the experimental isotherms, using the generalized eq 3. The theoretical lines provide an excellent fit to the experimental isotherms with the values of $K = (2.8 \pm 0.5) \times 10^5$ M^{-1} and $\omega = 1.5 \pm 0.5$ (Table 1). The corresponding parameters, previously determined for the modified domain, are $K = (2.7 \pm 0.5) \times 10^5$ M^{-1} and $\omega = 4 \pm 1$ (*22*). Thus, the presence of an additional, positively charged lysine residue has, within experimental accuracy, no effect on the intrinsic binding constant in the examined solution conditions, although parameter ω which characterizes cooperative interactions is decreased by a factor of ~2.5 (Table 1).

Salt Effect on Intrinsic Affinity of the Rat Pol β 8-kDa Domain−ssDNA Complex. Fluorescence titrations of poly(dϵA) with the 8-kDa domain of rat pol β, in buffer C1 (pH 7.0, 10 °C), containing different NaCl concentrations, are shown in Figure 3a. As the salt concentration increases, the isotherms shift toward higher total protein concentrations, indicating a decreasing macroscopic affinity of the domain−nucleic acid complex at higher salt concentrations. Also, the maximum relative fluorescence change accompanying the binding decreases with the increase of the salt concentration (Figure 3a). Analogous fluorescence titrations were performed in the solutions where NaCl was replaced by NaBr (data not shown).

The dependence of the logarithm of the intrinsic binding constant upon the logarithm of [NaCl] and [NaBr] (log−log plots) is shown in Figure 3b (*40*−*42*). Both plots are linear in the studied salt concentration range. In the presence of NaCl, the slope of the plot, $\partial \log K/\partial \log [NaCl]$, is -4.8 ± 0.5, which indicates that the release of ~5 ions accompanies the intrinsic interactions between the domain and the ssDNA. The slope, $\partial \log K/\partial \log [NaBr] = -4.5 \pm 0.5$ is very similar to the slope obtained in the presence of NaCl. Also, the determined binding constants have very close values in both salts. Thus, the replacement of Cl^- by Br^- does not significantly affect the number of ions released in the formation of the complex or the values of the intrinsic binding constants. Br^- anions are known to have a higher affinity for the protein amine groups than Cl^- (*43*). Independence of the net number of ions released, as well as the values of binding constants, upon the type of the anion strongly suggests that intrinsic interactions are predominantly accompanied by the release of cations from the nucleic acid (*40*−*42*) (see Discussion).

The salt effect on the domain interactions with the ssDNA is different in the presence of Mg^{2+}. Fluorescence titrations of poly(dϵA) with the 8-kDa domain of rat pol β, in buffer C (pH 7.0, 10 °C), containing different NaCl concentrations, are shown in Figure 4a. Analogous titrations have been performed in the presence of NaBr (data not shown). The

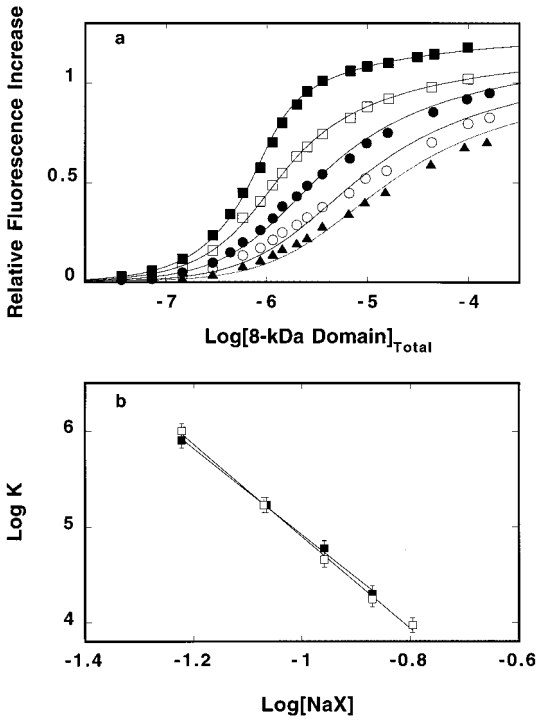

FIGURE 3: (a) Fluorescence titrations of poly(dϵA) (λ_{ex} = 325 nm, λ_{em} = 410 nm) with the 8-kDa domain of rat pol β in buffer C1 (pH 7.0, 10 °C) containing different NaCl concentrations: (■) 50 mM; (□) 75 mM; (●) 100 mM; (○) 125 mM; (▲) 150 mM. The solid lines are computer fits of the binding isotherms using the generalized McGhee−von Hippel model, as defined by eq 3. The concentration of poly(dϵA) is 2×10^{-5} M (nucleotide). (b) Dependence of the intrinsic binding constants, *K*, for the binding of the 8-kDa domain of rat pol β to poly(dϵA) upon NaCl (■) and NaBr (□) concentrations (log−log plots). The plots are characterized by the slopes $\partial \log K/\partial \log [\mathrm{NaCl}] = -4.8 \pm 0.5$, and $\partial \log K/\partial \log [\mathrm{NaBr}] = -4.5 \pm 0.5$, respectively.

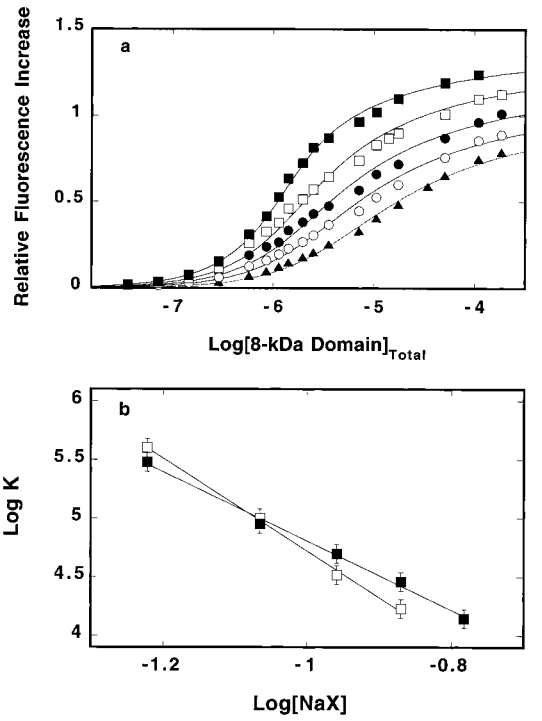

FIGURE 4: (a) Fluorescence titrations of poly(dϵA) (λ_{ex} = 325 nm, λ_{em} = 410 nm) with the 8-kDa domain of rat pol β in buffer C (pH 7.0, 10 °C), containing 1 mM $MgCl_2$ and different NaCl concentrations: (■) 50 mM; (□) 75 mM; (●) 100 mM; (○) 125 mM; (▲) 150 mM. The solid lines are computer fits of the binding isotherms using the generalized McGhee−von Hippel model, as defined by eq 3. The concentration of poly(dϵA) is 2×10^{-5} M (nucleotide). (b) Dependence of the intrinsic binding constant, *K*, for the binding of the 8-kDa domain of rat pol β to poly(dϵA) upon NaCl (■) and NaBr (□) concentrations (log−log plots). The plots are characterized by the slopes $\partial \log K/\partial \log [\mathrm{NaCl}], = -2.9 \pm 0.5$ and $\partial \log K/\partial \log [\mathrm{NaBr}] = -4 \pm 0.5$, respectively.

solid lines are computer fits of the experimental titration curves using the generalized McGhee−von Hippel equation (eq 3). The dependence of the logarithm of the intrinsic binding constant upon the logarithm of [NaCl] and [NaBr] is shown in Figure 4b. Within experimental accuracy, the plots are linear in the studied salt concentration range and characterized by the slopes $\partial \log K/\partial \log [\mathrm{NaCl}] = -2.9 \pm 0.5$ and $\partial \log K/\partial \log [\mathrm{NaBr}] = -4 \pm 0.5$, respectively.

The values of the binding constants and both slopes are reduced in the presence of Mg^{2+}. This results from the fact that both the protein and magnesium ions compete for the same binding site on the nucleic acid. Moreover, bound magnesium cations reduce the thermodynamic degree of Na^+ binding to the DNA which, in consequence, reduces the number of sodium ions released upon protein binding and the absolute values of the slopes of the log−log plots, as experimentally observed (*40*−*42*). However, the slope of the log−log plot, in the presence of NaBr, is significantly larger than the corresponding slope obtained in the presence of NaCl (Figure 4b), indicating that the replacement of Cl^- by Br^- increases the net ion release. Thus, the presence of $MgCl_2$ dramatically changes the salt effect on the 8-kDa domain−ssDNA interactions (see Discussion).

A quantitative determination of the salt effect on the cooperativity parameter ω is more difficult because of the small value of the parameter and the inherent large error in its determinations. Nevertheless, the obtained values of the slopes $\partial \log \omega/\partial \log [\mathrm{NaCl}]$ are -1 ± 0.5 and -0.8 ± 0.4, in the absence and presence of $MgCl_2$. The analogous values of the slopes, $\partial \log \omega/\partial \log [\mathrm{NaBr}]$, are -1 ± 0.5 and -0.6 ± 0.3, respectively (data not shown). These data indicate that cooperative interactions are accompanied by a net release of ~1 ion that is not, within experimental accuracy, affected by the presence of Mg^{2+}.

Binding of the Rat Pol β 8-kDa Domain to the ssDNA Oligomers Having a Different Number of Nucleotide Residues. The total site size of a protein−DNA complex corresponds to the DNA fragment that is prevented from binding to other protein molecules (*37*−*39*). Such DNA fragments may include nucleotide residues directly involved in interactions with the protein, its DNA-binding site, and nucleotides not engaged in direct interactions (*34*). The latter are prevented from interacting with another protein molecule by the protruding protein matrix of the previously bound protein molecule over nucleotides adjacent to the binding site (*34*).

A deeper insight into the structure of the 8-kDa domain DNA-binding site can be obtained by examining the interactions of the domain with the ssDNA oligomers that have a different number of nucleotide residues. We previously applied a similar strategy in our studies of the ssDNA-binding sites of the *Escherichia coli* DnaB and PriA helicases (*34*, *44*). Fluorescence titrations of the 12-, 10-, 9-, 8-, 6-, and 5-mer, dϵA(pϵA)$_{11}$, dϵA(pϵA)$_9$, dϵA(pϵA)$_8$, dϵA(pϵA)$_7$, dϵA-

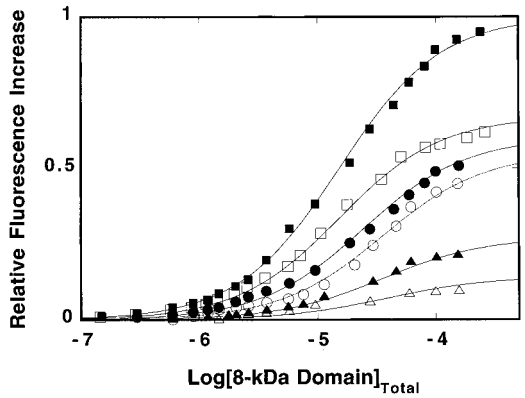

FIGURE 5: Fluorescence titrations of the 12-, 10-, 9-, 8-, 6-, and 5-mer, dϵA(pϵA)$_{11}$, dϵA(pϵA)$_9$, dϵA(pϵA)$_8$, dϵA(pϵA)$_7$, dϵA(pϵA)$_5$, and dϵA(pϵA)$_4$ (λ_{ex} = 325 nm, λ_{em} = 410 nm), with the 8-kDa domain of rat pol β in buffer C (pH 8.1, 10 °C), containing 50 mM NaCl. Concentrations of all oligomers are 4.5×10^{-7} M (oligomer): (■) dϵA(pϵA)$_{11}$; (□) dϵA(pϵA)$_9$; (●) dϵA(pϵA)$_8$; (○) dϵA(pϵA)$_7$; (▲)dϵA(pϵA)$_5$; (△) dϵA(pϵA)$_4$. The solid lines are computer fits using the single-site binding isotherm, $\Delta F = \Delta F_{max}$-$[K_N P_F/(1 + K_N P_F)]$, with binding parameters K_N and ΔF_{max} included in Table 2.

(pϵA)$_5$, and dϵA(pϵA)$_4$, with the 8-kDa domain in buffer C (pH 7.0, 10 °C), containing 50 mM NaCl, are shown in Figure 5. The solid lines are computer fits of the binding isotherms to a single binding-site isotherm, $\Delta F = \Delta F_{max} K_N P_F/(1 + K_N P_F)$, where ΔF_{max} is the maximum fluorescence increase and K_N is the macroscopic binding constant for a given oligomer. It should be pointed out that in the case of the short ssDNA oligomers (4- and 5-mer), at saturation with the DNA, two molecules of the nucleic acid may bind to the domain. The low fluorescence increase, observed for the short oligomers, makes the maximum stoichiometry determination very difficult. However, the low DNA concentrations applied here and the reverse titration mode (increasing protein concentration) of performing the experiments make such saturation very improbable. Nevertheless, the macroscopic binding constants for these two oligomers may contain a statistical factor no higher than 2. The obtained binding parameters are included in Table 2.

There are two characteristic features of the 8-kDa domain interactions with different ssDNA oligomers. The maximum fluorescence increase, ΔF_{max}, dramatically decreases with the decreasing length of the oligomer. Such ΔF_{max} changes indicate a changing ssDNA structure in the complex with the protein (*45*, *46*; see Discussion). However, the macroscopic binding constant for the examined oligomers only gradually decreases with the size of the oligomer (Table 2). These results contrast the data obtained for the ssDNA-binding sites of the DnaB and PriA helicases, where a sharp drop of both ΔF_{max} and macroscopic affinities occurred, when the number of nucleotides was lower than a certain limit, indicating that below this specific length the DNA was not able to interact with crucial contacts in the binding site (*34*, *44*). Very different behavior observed for the 8-kDa domain strongly suggests that its DNA-binding site has a continuous, energetically homogeneous structure with multiple contacts between the protein and the DNA instead of a small number of key contacts separated by a specific distance (see Discussion).

Base Specificity in the Rat Pol β 8-kDa Domain−ssDNA Interactions. Using the MCT method outlined in the Materials and Methods section, we can quantitatively address the base specificity in interactions of the rat pol β 8-kDa domain with various unmodified polynucleotides, differing by the type of the base (*27*). In these studies we use poly(dϵA) as a reference, fluorescence nucleic acid. A fluorescence titration of the poly(dϵA) [2×10^{-5} M (nucleotide)] with the 8-kDa domain in the presence of poly(dT) [3.11×10^{-5} M (nucleotide)] in buffer C (pH 7.0, 10 °C), containing 50 mM NaCl, is shown in Figure 6a. For comparison, we also include the titration curve of only poly(dϵA) with the domain, at the same fluorescent nucleic acid concentration as in the titration performed in the presence of poly(dT). In the presence of the competing, nonfluorescent poly(dT), the binding isotherm is shifted toward higher protein concentrations, due to the simultaneous binding of the protein to the poly(dϵA) and the unmodified polynucleotide. On the other hand, at the same value of the fluorescence increase of poly(dϵA), independently of the presence of the competing poly(dT), the physical state of the fluorescent nucleic acid must be the same, i.e., the values of $\sum \nu_i$ and the free protein concentration [8-kDa domain]$_F$ must be the same (*27*). The binding density of the protein on the competing, unmodified ssDNA, $(\sum \nu_i)_S$, is also a sole, unique function of the [8-kDa domain]$_F$. Therefore, at a given value of fluorescence increase, the value of $(\sum \nu_i)_S$ must be the same, independent of the concentration of the unmodified nucleic acid. The binding density, $(\sum \nu_i)_S$, can then be obtained using eq 5a (*27*).

The dependence of the fluorescence increase of the reference poly(dϵA), as a function of the average binding density, $(\sum \nu_i)_S$, of the 8-kDa domain−poly(dT) complex, is shown in Figure 6b. The plot is concave up, showing that in the low concentration range the domain binds predominantly to poly(dT). In other words, this behavior indicates that the 8-kDa domain has a higher affinity for the competing lattice than for the reference poly(dϵA) (*27*). Short extrapolation to the maximum observed fluorescence change gives $(\sum \nu_i)_S = 0.11 \pm 0.007$, which indicates that the site size of the 8-kDa domain complex with poly(dT) is, within experimental accuracy, the same as that obtained for poly(dϵA) (Table 1). The solid line in Figure 6a is the computer fit of the simultaneous binding of the 8-kDa domain to two competing nucleic acids, using the procedure for fitting the isotherm of a large ligand binding to two competing nucleic acid lattices, as outlined in Materials and Methods (*27*). The binding of the domain to poly(dϵA) has been described, using the generalized McGhee−von Hippel equation (eq 3) with the independently determined $K = 2.8 \times 10^5$ M^{-1}, $\omega = 1.5$, and $n = 9$. The binding of the domain to poly(dT) is described by eqs 6 and 7. There are only two parameters, the intrinsic binding constant, K_S, and the cooperativity parameter, ω_S, remaining to be determined. The best fit of the experimental isotherm is obtained with $K_S = (1.6 \pm 0.5) \times 10^6$ M^{-1} and $\omega_S = 5 \pm 1.5$. The solid line in Figure 6b is the computer simulation of the observed fluorescence change of the reference poly(dϵA), as a function of the degree of binding of the 8-kDa domain on poly(dT), using the determined binding parameters for poly(dϵA) and the unmodified ssDNA polymer. The parameters for all studied ssDNA polymers are included in Table 3. Although the 8-kDa domain shows some preference for poly(dT) among studied ssDNA polymers, its affinities for different ssDNAs

Table 2: Macroscopic Binding Constant, K_N, and Maximum Fluorescence Change, ΔF_{max}, for Rat Pol β 8-kDa Domain Binding to ssDNA Oligomers with a Different Number of Nucleotide Residues in Buffer C (pH 7.0, 10 °C), Containing 50 mM NaCl[a]

parameter	12-mer dϵA(pϵA)$_{11}$	10-mer dϵA(pϵA)$_9$	9-mer dϵA(pϵA)$_8$	8-mer dϵA(pϵA)$_7$	6-mer dϵA(pϵA)$_5$	5-mer dϵA(pϵA)$_4$
K_N (M^{-1})	$(6.8 \pm 2) \times 10^4$	$(6.8 \pm 2) \times 10^4$	$(4.2 \pm 1.5) \times 10^4$	$(2.9 \pm 1) \times 10^4$	$(2.9 \pm 1) \times 10^4$	$(2.8 \pm 1) \times 10^4$
ΔF_{max}	1 ± 0.1	0.67 ± 0.05	0.6 ± 0.05	0.55 ± 0.05	0.27 ± 0.03	0.14 ± 0.02

[a] Errors are standard deviations determined using three to four independent titration experiments.

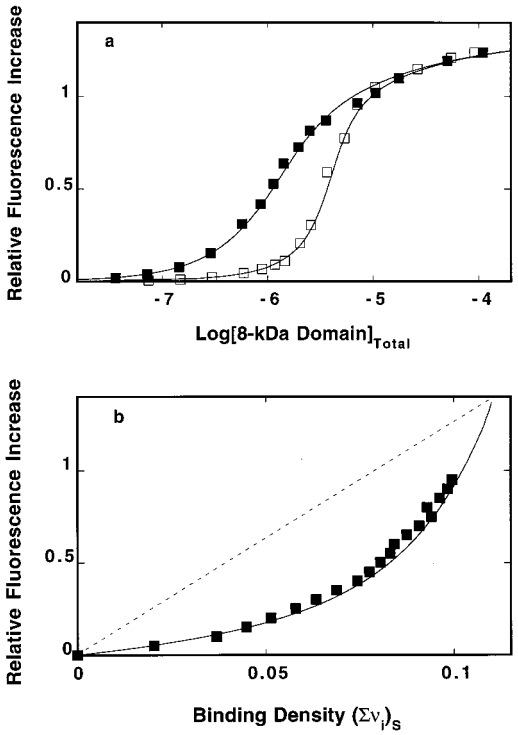

FIGURE 6: (a) Fluorescence titrations of poly(dϵA) ($\lambda_{ex} = 325$ nm, $\lambda_{em} = 410$ nm) with the 8-kDa domain of pol β in buffer C (pH 7.0, 10 °C), containing 50 mM NaCl, in the presence of poly(dT) (□). For comparison, the fluorescence titration of only poly(dϵA), in the same solution conditions, is included (■). The solid line is the computer fit of the experimental fluorescence binding isotherms using the lattice competition titration approach described in the Materials and Methods section. The binding parameters are included in Table 3. The concentrations of poly(dϵA) and poly(dT) are 2×10^{-5} and 3.11×10^{-5} M (nucleotide), respectively. (b) Dependence of the observed fluorescence increase of poly(dϵA) upon the binding density, $(\Sigma\nu_i)_S$, of the 8-kDa domain−poly(dT) complex (■). The quantitative determination of $(\Sigma\nu_i)_S$ has been performed using the MCT method described in Materials and Methods (*27*, *34*). The solid line is the computer simulation of the dependence of ΔF upon $(\Sigma\nu_i)_S$, using the determined binding parameters for both nucleic acid lattices (Table 3). The dashed line is the dependence of ΔF upon $\Sigma\nu_i$ of the protein on poly(dϵA) in the absence of the competing poly(dT).

are characterized by similar intrinsic binding constants and cooperativity parameters (Table 3).

Binding of the 8-kDa Domain to the dsDNA. Site Size, Intrinsic Affinity, and Cooperativity. Using the MCT method, in an analogous way, as described above, we can quantitatively examine the interactions of the 8-kDa domain with the dsDNA (*27*). The persistent length of the dsDNA is much larger than the persistent length of the ssDNA. For instance, in the presence of Mg^{2+}, we do not expect the site size of the domain−dsDNA complex to be larger than the value determined for the ssDNA, i.e., $n = 9 \pm 0.6$ base pairs (see above). This conclusion is fully supported by the examination of the binding of the 8-kDa domain to the dsDNA oligomer that contains 10 bps of random sequence (data not shown). A single domain molecule binds to the oligomer, indicating that the site size of the complex with the dsDNA is close to the site size determined for the ssDNA (Tables 1 and 2). To further address the site size, intrinsic affinity, and cooperativity in the binding of the 8-kDa domain to the dsDNA, the experiments were performed with the 20-mer dsDNA having a random sequence. As in the previous section, we used poly(dϵA) as a reference fluorescent nucleic acid.

Fluorescence titrations of poly(dϵA) with the 8-kDa domain, in the presence of the dsDNA oligomer [2.56×10^{-6} M (oligomer)], having 20 bps of random sequence, in buffer C (pH 7.0, 10 °C), containing 50 mM NaCl, are shown in Figure 7a. For comparison, the titration of poly(dϵA) alone is also included. The presence of the dsDNA oligomer significantly shifts the titration curves toward a higher domain concentration range, clearly indicating that the dsDNA oligomer efficiently competes with the polymer ssDNA for the same DNA-binding site on the protein. However, we could not reach the maximum possible plateau of the titration curve because, at a higher protein concentration, precipitation of the protein−nucleic acid complex occurs. The isotherm presented in Figure 7a contains all points where the precipitation is not present.

The dependence of the relative fluorescence increase, as a function of the number of bound domain molecules per 20-mer dsDNA, $\sum\Theta_i$, is shown in Figure 7b. The average degree of 8-kDa domain binding on the oligomer has been quantitatively determined, using the approach described in Materials and Methods (*27*, *34*). The behavior of the plot is very complex. It rises very sharply at low values of the degree of binding, then levels off at intermediate values of $\sum\Theta_i$, and rises once again at higher values of $\sum\Theta_i$. As we discussed before, such behavior of the plot indicates that the macroscopic affinity of the 20-mer is higher than the affinity for the polymer ssDNA (*27*). Moreover, contrary to the complexes with the ssDNA, the binding of the domain to the dsDNA must be characterized by significant positive cooperativity (*27*). The determined maximum value of $\sum\Theta_i$ is 1.9 ± 0.1. Although extrapolation of the final slope of the plot to the maximum possible value of the fluorescence increase, $\Delta F_{max} = 1.4$, provides the stoichiometry of 2.5 ± 0.3, the complex behavior of the plot makes such extrapolation rather inaccurate for the considered case (*27*). The determination of all binding parameters has been accomplished by the simultaneous analysis of both plots in Figure 7.

In the studied binding system, we have a single ligand, the 8-kDa domain, competing for two different nucleic acids, poly(dϵA) and the 20-mer dsDNA. Binding to poly(dϵA) is described by eq 3, with the independently determined $K = 2.8 \times 10^5$ M^{-1}, $\omega = 1.5$, and $n = 9$ (Table 1). Assuming that a maximum of two domain molecules bind to the 20-

Table 3: Intrinsic Binding Constant, K, Cooperative Interaction Parameter, ω, and Site Size, n, for Rat Pol β 8-kDa Domain Binding to ssDNA Homopolymers in Buffer C (pH 7.0, 10 °C), Containing 50 mM NaCl[a]

parameter	poly(dϵA)	poly(dA)	poly(dT)	poly(dC)
K (M^{-1})	$(2.8 \pm 0.5) \times 10^5$	$(1.4 \pm 0.8) \times 10^5$	$(1.6 \pm 0.5) \times 10^6$	$(2.1 \pm 0.7) \times 10^5$
ω	1.5 ± 0.5	5 ± 2	5 ± 1.5	2.5 ± 1
n	9 ± 0.6	9 ± 0.6	9 ± 0.6	9 ± 0.6

[a] Errors are standard deviations determined using three to four independent titration experiments.

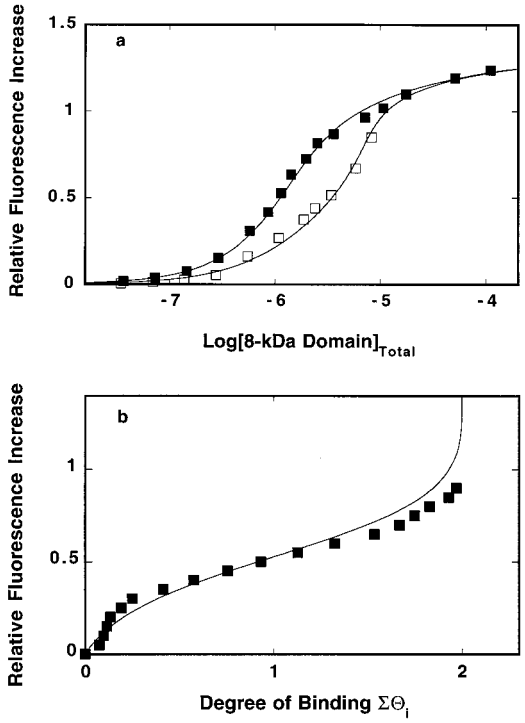

FIGURE 7: (a) Fluorescence titrations of poly(dϵA) ($\lambda_{ex} = 325$ nm, $\lambda_{em} = 410$ nm) with the rat pol β 8-kDa domain in buffer C (pH 7.0, 10 °C), containing 50 mM NaCl, in the presence of the dsDNA 20-mer (5′-GCAGGCTCGTTACGTGATGC-3′:3′-CGTCCGAGCAATGCACTACG-5′) (□). For comparison, the fluorescence titration of only the poly(dϵA), in the same solution conditions, is included (■). The solid line is the computer fit of the experimental fluorescence binding isotherm using the lattice competition titration approach described in Materials and Methods and specifically defined for this case by eqs 8−10. The fit is performed using binding parameters independently determined for poly(dϵA) (Table 3) and $K_{DS} = 4 \times 10^5$ M^{-1}, $\omega_{DS} = 90$. The concentrations of poly(dϵA) and the dsDNA 20-mer are 2×10^{-5} (nucleotide) and 2.56×10^{-6} M (oligomer), respectively. (b) Dependence of the observed fluorescence increase of poly(dϵA) upon the average degree of binding, $\Sigma\Theta_i$, of the 8-kDa domain−dsDNA 20-mer complex (■). The quantitative determination of $\Sigma\Theta_i$ has been performed using the MCT method described in Materials and Methods (*23*, *27*, *34*). The solid line is the computer simulation of the dependence of ΔF upon $\Sigma\Theta_i$ using the determined binding parameters for both nucleic acids. The dashed line is the dependence of ΔF upon $\Sigma\nu_i$ of the protein on poly(dϵA) in the absence of the competing dsDNA oligomer.

mer, and using the same site size of the 8-kDa domain−dsDNA complex as determined for the ssDNA, i.e., $n = 9$, the binding of two domain molecules to the dsDNA 20-mer is described by the partition function, Z_{20}, as

$$Z_{20} = 1 + (N - n + 1)K_{DS}P_F + K_{DS}\omega_{DS}P_F^2 \quad (8a)$$

and the degree of binding, $\sum\Theta_i$, of the 8-kDa domain on the dsDNA 20-mer is

$$\sum\Theta_i = \frac{(N - n + 1)K_{DS}P_F + 2K_{DS}\omega_{DS}P_F^2}{Z_{20}} \quad (8b)$$

where N is the number of the base pairs in the dsDNA (in our case $N = 20$), K_{DS} is the intrinsic binding constant for the dsDNA 20-mer, ω_{DS} is the parameter characterizing cooperative interactions between the bound 8-kDa domain molecules, and P_F is the free concentration of the 8-kDa domain. The concentration of the bound 8-kDa domain to both nucleic acids is then

$$P_b = (\sum \nu_i)N_T + (\sum \Theta_i)N_{20_T} \quad (9)$$

where N_T and N_{20_T} are the total concentrations of poly(dϵA) (nucleotide) and the dsDNA 20-mer (oligomer), respectively, and $\sum\nu_i$ is defined by eq 3. The concentration of the bound domain, P_b, is related to the total domain concentration, P_T, by the mass conservation equation

$$P_T = P_F + P_b \quad (10)$$

The solid line in Figure 7a is a nonlinear least-squares fit of the experimental isotherm using eqs 8−10, with two fitting parameters, K_{DS} and ω_{DS}. The obtained values are $K_{DS} = (4 \pm 1) \times 10^5$ M^{-1} and $\omega_{DS} = 90 \pm 30$, respectively. Thus, with the exception of poly(dT), the intrinsic dsDNA affinity of the 8-kDa domain is higher than its intrinsic affinities for the studied ssDNA polymers (Table 3). A similar value of $K = (3 \pm 0.6) \times 10^5$ M^{-1} has been obtained for the dsDNA 10-mer, corresponding to the first half of the studied 20-mer (Figure 7a), indicating that the possible "end effect" is negligible in 8-kDa domain interactions with the dsDNA. On the other hand, the value of the cooperativity parameter, ω_{DS}, is much higher than the values of ω determined for the ssDNAs (Table 3).

The solid line in Figure 7b is the computer simulation of the observed fluorescence change of the reference poly(dϵA), as a function of the degree of binding of the 8-kDa domain on the dsDNA 20-mer, using the determined binding parameters for poly(dϵA) and the dsDNA oligomer. The theoretical line provides an adequate description of the complex, experimental isotherm indicating correctness of all binding parameters, including the site size $n = 9$ bps. It is evident that the complex behavior of the plot results from the significant cooperative interactions between the 8-kDa domain molecules bound to the 20-mer, resulting in a sharp rise of the plot with the binding of the second molecule of the domain to the 20-mer at a high protein concentration range.

DISCUSSION

Studies described in this work provide, for the first time, an insight into the complex energetics of the native rat pol

β 8-kDa domain complexes with DNA. The experiments were performed with an isolated domain that allowed us to characterize the DNA-binding site of the domain without any interference from the remaining part of the enzyme molecule. The examination of the interactions was possible due to the application of the quantitative fluorescence titration technique (*32*−*36*). This approach allowed us to determine the binding density, or the degree of binding, of a protein−DNA complex, over a large protein concentration range, without any assumption as to the relationship between the observed signal used to monitor the binding and the stoichiometry of the studied complexes (*32*−*36*).

The Site Size of the 8-kDa Domain−ssDNA Complex Is Much Larger Than the Site Size of the (Pol β)$_5$ Binding Mode of the Intact Rat Pol β. As we mentioned above, the total site size of a protein−DNA complex corresponds to the number of nucleotide residues, or base pairs, which are prevented from binding to other protein molecules (*37*−*39*). This fundamental quantity, characterizing a protein−nucleic acid complex, is crucial for any quantitative analysis of the mechanism of the functioning of the protein (*27*). A striking feature of the isolated 8-kDa domain−ssDNA complex is the large site size, *n*, of the complex. In the absence of Mg^{2+}, the value of *n* is 13 ± 0.7, as compared to the site size $n = 5 \pm 2$, which has been determined for the (pol β)$_5$ binding mode. These data clearly show that the ssDNA-binding site of the domain is much larger than indicated by the site size of the (pol β)$_5$ binding mode. However, the total site size may include the number of nucleotide residues which engage in direct interactions with the actual ssDNA-binding site of the protein, as well as residues that are sterically prevented from interacting with another protein molecule, simply by the protruding protein matrix of the bound protein. This is the case for the ssDNA-binding sites of the *E. coli* DnaB and PriA helicases previously examined by us (*34*, *44*). Although both helicases have the total ssDNA site size of 20 ± 3 nucleotide residues, the experiments with a series of ssDNA oligomers indicated that the actual ssDNA-binding sites require only 7 ± 1 and 8 ± 1, respectively, to provide affinities similar to the intrinsic affinities of the total site sizes (*34*, *44*). Thus, the affinity of the ssDNA oligomers, shorter by 1 or 2 residues than the size of the ssDNA-binding site, dropped dramatically to an undetectable level (*34*, *44*). In other words, such experiments indicate that crucial contacts between the proteins and the ssDNA, necessary to generate the free energy of binding similar to the affinity for the total site size, are separated by a precise, specific distance (*34*, *44*).

The behavior of the DNA-binding site of the 8-kDa domain, in experiments with different ssDNA oligomers, is more complex. The macroscopic affinity between the 12-mer and 5-mer gradually decreases, which would suggest that the crucial contacts between the protein and the nucleic acid are not separated by more than 3−5 nucleotide residues. However, the observed maximum fluorescence increase, ΔF_{max}, decreases by a factor of ∼7 from ∼1 to ∼0.14 between the 12- and 5-mer, respectively. Such a dramatic ΔF_{max} decrease with only a moderate decrease of the macroscopic affinity has never been observed before (*34*, *44*).

The fluorescence of ϵA in the etheno derivatives of the polymer and oligomer nucleic acids is predominantly affected by the mobility and separation of the bases and not by the polarity of the environment (*28*, *34*, *45*, *46*). The large decrease of ΔF_{max} indicates a much less rigid conformation of the ssDNA in the complex between the domain and the 5-mer than in the complex with the 12-mer, despite the similar macroscopic affinities (Table 2). The plausible explanation of this behavior is that the DNA-binding site of the 8-kDa domain has a continuous, energetically homogeneous structure with similar multiple contacts spread evenly over the entire binding site that encompasses 13 ± 0.7 nucleotide residues. These contacts in the binding site provide a similar weight to the free energy of binding. Notice, this would suggest that a much higher affinity for, e.g., the 12-mer than for the 5-mer should be observed, because a larger number of contacts is formed between the protein and the longer oligomer. However, much more pronounced conformational changes of the 12-mer in the complex with the protein strongly suggest that part of the free energy of the 12-mer binding is used for conformational adjustments of the longer oligomer to the structure of the entire binding site. The larger base separation and immobilization will certainly lead to the much larger value of ΔF_{max} (1 ± 0.1) than the corresponding ΔF_{max} observed for the 5-mer (0.14 ± 0.02) (Table 2; Figure 5). Such conformational changes, not induced in the case of shorter oligomers, can result in a significant reduction of macroscopic affinities of the longer nucleic acids to a level similar to the shorter ssDNAs, as experimentally observed.

Strong support for the proposed continuous, energetically homogeneous structure of the 8-kDa domain DNA-binding site, with a large number of contacts between the protein and the ssDNA, comes from the salt effect on the observed intrinsic affinity of the 8-kDa domain−ssDNA complex. The data obtained in the absence of magnesium are of particular importance because complications resulting from the presence of the additional competing Mg^{2+} ligand are eliminated (*40*−*42*). Formation of the complex is accompanied by the net release of ∼5 ions (Figure 3). Changing the pH by an entire unit (7 to 8.1) does not significantly affect the intrinsic ssDNA affinity of the domain (data not shown). Such independence indicates that proton release and/or uptake does not contribute to the observed ion release in the examined pH range (*40*, *41*); i.e., increasing the salt concentration predominantly affects only cation and anion exchange.

The slope of the log−log plot for the protein−nucleic acid interactions can then be defined by the linkage relationship, $\partial \log K_N / \partial \log [NaCl] = -p - q$, where *p* and *q* are the average net numbers of cations and anions released upon the complex formation (*40*−*42*). Taking into account the thermodynamic degree of cation binding per phosphate group of the ssDNA, ψ, the slope of the log−log plot is defined by the linkage relationship, $\partial \log K / \partial \log[NaCl] = -m\psi - q$, where *m* is the number of ionic interactions between the protein and the nucleic acid (*42*, *43*). The fact that the number of ions released, as well as the values of intrinsic binding constants, is independent of the type of anion in solution indicates that only cations from the ssDNA are being released upon complex formation; i.e., the expression for the slope reduces to $\partial \log K / \partial \log [NaCl] = -m\psi$. Using the value of $\psi = 0.71$, determined for the ssDNA, provides the value of $m = 6.8 \pm 0.5$ (*40*, *41*). Thus, with the assumption of no proton release or uptake, the obtained data strongly suggest

that as many as ∼7 ionic contacts are formed between the 8-kDa domain and the DNA and these nonspecific, electrostatic interactions dominate the free energy of the binding process.

It is interesting to compare the results of the thermodynamic studies reported in this work, which indicate a continuous, energetically homogeneous DNA-binding site of the 8-kDa domain with multiple interaction contacts, with the known crystal and NMR structures of the domain (*17*−*19*). The domain contains a helix−hairpin−helix motif (HhH) which is proposed to be a nonspecific, ssDNA-binding motif (*47*, *48*). The motif contains two α-helices connected by a short interhelical loop (*47*). In fact, the pol β complex with the ssDNA is the only currently determined structure of the HhH−DNA complex (*6*, *19*). In the presence of the ssDNA, the loop can make contact with the two nucleic acid phosphate groups via hydrogen bonds. It is clear that the motif alone, although a part of the binding site, cannot account for either the site size of 13 or 9 nucleotide residues or for the ∼7 ionic interactions between the domain and the nucleic acid.

The 8-kDa domain contains 17 lysine and arginine residues (*6*, *9*). On both sides of the HhH motif there is a path of 8−7 lysines and arginines. Each of these patches, together with the HhH loop, can form a DNA-binding site that would account for the determined site size and ∼7 ionic interactions. Some of these residues, including lysines K41, K60, K68, and K72 and arginines R40 and R83, were indeed implicated in interactions with the ssDNA in excellent and extensive NMR studies of the isolated 8-kDa domain complex with the DNA (*17*, *48*). Notice that the net number of ions released upon complex formation between the modified 8-kDa domain, which contains asparagine in location 87, and the native domain, which contains lysine in location 87, are -1.9 ± 0.5 and -2.9 ± 0.5, respectively (Figure 4b; *22*). Although these values were determined in the presence of Mg^{2+}, the much larger value obtained for the unmodified domain strongly suggests that the lysine residue in location 87 is engaged in interactions with the ssDNA. Lysines 72 and 68 and tyrosine 39 were proposed to be part of the active site of the domain for the excision of the deoxyribose phosphate from the 5′-incised apurinic/apyrimidinic site during base excision repair (*6*, *14*). This does not exclude them from being a part of the DNA-binding site. On the contrary, it indicates that during the excision process the 5′ terminus of the nucleic acid is placed in the direct vicinity of these residues. Thus, these data and NMR studies strongly suggest that the DNA-binding site is located at the C-terminal side of the HhH motif.

In the context of the energetically homogeneous binding site, the remaining question is: why is the site size of the domain not changing when the binding density of the domain on the ssDNA increases? In other words, why is the transition between the ssDNA-binding modes observed only for the intact pol β? As we mentioned above, binding of the longer ssDNA oligomers to the 8-kDa domain is characterized by the dramatically larger fluorescence changes, as compared to the shorter oligomers, indicating strong immobilization and separation between the bases imposed by the structure of the entire DNA-binding site (Figure 5). These data indicate that the imposed orientation of the nucleic acid in the binding site is different for the oligomers with different lengths. The lack of the site size changes in the case of the isolated domain may result from the fact that, in order to bind the polymer ssDNA, using a smaller site size, the entire domain would have to change its orientation with respect to the nucleic acid. Such complexes could induce negative cooperative interactions between the domain molecules not present in the case of the intact enzyme and which cannot be overcome by the negative lattice entropy favoring a smaller site size (*37*−*39*). As result, the binding mode transition is the intrinsic property of the intact enzyme and not its isolated 8-kDa domain, although both share the same DNA-binding site.

Specific Magnesium Binding to the 8-kDa Domain Affects the Site Size of the Domain−ssDNA Complex. In the presence of Mg^{2+}, the total site size of the 8-kDa domain complex with the ssDNA is reduced to 9 ± 0.6 (Figures 1 and 2). The effect is completely saturated at the $MgCl_2$ concentration of ∼1 mM, indicating that cation binding sites participating in the process are characterized by the binding constant $\geq 10^4$ M^{-1}. Such high affinity indicates that, in our solution conditions, [NaCl] > 0.1 M, the observed decrease of the site size is induced by magnesium binding to the protein and not to the ssDNA (*42*).

Additional evidence that the magnesium effect results from the cation binding to the protein comes from the observed changes in the net ion release accompanying the 8-kDa domain−ssDNA complex formation in the presence of $MgCl_2$. As we discussed above, the decrease of the net number of ions released is an expected result, because of the reduced level of Na^+ condensation of the DNA (*40*−*42*). However, there is a clear dependence of the net number of ions released on the type of anion in solution. In the presence of Br^- the slope $\partial \log K/\partial \log[\text{NaBr}]$, is -4 ± 0.5 as compared to -2.9 ± 0.5 observed in the presence of only Cl^- (Figure 2b). Because bromide ions have a significantly higher affinity for the protein amine groups than Cl^- (*44*), these data strongly suggest that, as a result of magnesium binding, the protein acquires additional anion binding site(s). Thus, conformational changes induced by Mg^{2+} binding to the 8-kDa domain affect the protein−nucleic acid interface, resulting in an additional release of anions from the protein upon formation the complex with the nucleic acid.

The DNA-Binding Site of the 8-kDa Domain Has Low Base Specificity. Quantitative lattice competition studies, using the MCT method, show that the intrinsic binding constant of the 8-kDa domain for various ssDNA homopolymers differs, at most, by a factor of ∼5 (Table 3). These results show that the DNA-binding site of the domain has low base specificity; i.e., the bases contribute little to the free energy of the domain binding to the nucleic acid. As we discussed above, both salt dependence and experiments with different ssDNA oligomers strongly suggest that the domain−ssDNA recognition process is dominated by electrostatic interactions between the protein and the nucleic acid. In this context, low base specificity is in excellent agreement with the proposed nonspecific nature of interactions between the DNA-binding site and the DNA.

The value of the parameter ω characterizing cooperative interactions is very low and similar for all examined ssDNA polymers (Table 3). Thus, cooperative interactions are independent of the type of ssDNA base. In addition, it should be pointed out that the examined ssDNA polymers differ in

their structures. While poly(dA) and poly(dεA) have significant base stacking, poly(dT) has an unordered structure with very little stacking interactions between the bases (*49*). The independence of ω upon the type of base and the structure of the ssDNA polymer indicates that it characterizes intrinsic, weak protein−protein interactions between bound 8-kDa molecules (*22*, *23*).

The 8-kDa Domain−dsDNA Complex Has a Site Size and Intrinsic Affinity Similar to the Site Size and Intrinsic Affinity of the ssDNA. Because of its high affinity for the ssDNA, the 8-kDa domain was proposed to be a template-recognition domain, i.e., the domain that is exclusively responsible for recognition of the ssDNA conformation (*20*, *21*). However, quantitative studies described in this work clearly show that the domain has a significant intrinsic affinity for the dsDNA conformation. These results are in excellent agreement with the data previously obtained that indicated binding of the isolated 8-kDa domain to the dsDNA (*14*, *49*). In fact, with the exception of poly(dT), the intrinsic dsDNA affinity is even higher than the intrinsic affinities for the studied ssDNAs (Table 3). Thus, the DNA-binding site of the 8-kDa domain can accept both the ss and dsDNA conformation of the nucleic acid with comparable affinities. Such a lack of the more pronounced discrimination between these two different DNA conformations can be understood in the context of the proposed, nonspecific nature of the DNA-binding site of the 8-kDa domain discussed above.

The site size of the domain complex with the dsDNA, $n = 9 \pm 2$ bps, is, within experimental accuracy, the same as the site size determined for the complex with the ssDNA. Because of the significantly lower flexibility of the dsDNA, we expected a smaller site size (*48*). The similar value of n suggests that the domain may assume a different orientation when bound to the dsDNA, as compared to the complex with the more flexible ssDNA. Notice that the parameter $\omega_S = 90 \pm 30$, characterizing cooperative interactions, is much larger than the value of $\omega \approx 1.5-4$ determined for the ssDNAs (Tables 1 and 3). Such a different value of ω for the dsDNA conformation reinforces the conclusion that in the complex with the dsDNA the domain assumes a different orientation leading to significantly stronger interactions between the bound protein molecules. Further experiments are necessary to address this issue.

Functional Implications. When the availability of the ssDNA is decreased, rat pol β forms the (pol β)$_5$ binding mode, where the enzyme predominantly engages the small 8-kDa domain in interactions with the ssDNA, with a site size of 5 ± 2 nucleotide residues (*22*). Yet, the results described in this work clearly show that the DNA-binding site of the 8-kDa domain encompasses either 9 or 13 nucleotide residues, depending on the presence of Mg^{2+} cations. The large difference between the actual site size of the DNA-binding site and the site size of the (pol β)$_5$ binding mode indicates that the intact enzyme molecule is able to use only a part of the domain DNA-binding site. The partial use of the binding site can still generate enough free energy of binding to form a stable complex with the ssDNA, the (pol β)$_5$ binding mode. This is possible because of the continuous and energetically homogeneous structure of the binding site of the domain. Multiple interaction contacts in the site responsible for the generation of the free energy of binding are not clustered in a particular area nor are they separated by a specific distance, but evenly distributed throughout the binding site. Such ability to effectively use only part of the binding site provides the enzyme with a very efficient and specific mechanism to recognize small ssDNA gaps of a damaged DNA, independently of the gap size. Moreover, little dependence of the binding affinity upon the type of base and the nonspecific electrostatic character of binding ensures that every gap is recognized with similar efficiency. The dramatic effect of the Mg^{2+} cations on the site size of the 8-kDa domain complex with the ssDNA strongly suggests that the enzyme has the ability to change the topology of its DNA-binding site on the 8-kDa domain either through binding or through the release of magnesium cations. This ability would provide significant flexibility in adjusting to different structures of DNA substrates in the DNA repair processes.

The quantitative estimate of the site size and intrinsic dsDNA affinity of the 8-kDa domain, determined in this work, is of paramount importance. This affinity is still lower than the estimated affinity of the dsDNA-binding site located on the large 31-kDa domain of the protein (*21*; Jezewska et al., to be published). Therefore, the enzyme will predominantly bind the dsDNA using its large domain. However, in the complex with a gapped DNA having a small ssDNA gap with, e.g., 1−2 nucleotide residues, where the enzyme is bound to the gap with its large 31-kDa domain, only the dsDNA is available for the 8-kDa domain to bind. The obtained data suggest that the intact enzyme uses the intrinsic dsDNA affinity of the small 8-kDa domain to anchor itself at the gap. However, the site size of the complex with the dsDNA suggests that at least 9 bps, downstream from the primer, are required in order to efficiently anchor the enzyme at the gap. The fact that the DNA-binding site of the domain can accept ssDNA and dsDNA also indicates that, for intermediate ssDNA gaps, the domain can also simultaneously engage both the ssDNA and dsDNA of the DNA substrates, downstream from the primer.

In this context, the 8-kDa domain should not be considered as exclusively a template-binding domain, as initially proposed on the basis of its affinity for the ssDNA. By the same token, our previous results showed that the 31-kDa domain does not exclusively bind the dsDNA but can engage in interactions with the ssDNA in the (pol β)$_{16}$ binding mode (*22*, *23*). The obtained data and the discussion presented above indicate that the DNA-binding site located on the 8-kDa domain is an integral part of the total DNA-binding site of the polymerase which includes the part of the binding site located on the 31-kDa catalytic domain of the enzyme. Both DNA-binding subsites can engage different DNA conformations, depending on the structure of the DNA substrate and not because of their exclusive binding to one of the DNA conformations. Such ability is particularly important for the recognition of the gapped DNA in the damaged DNA. Our laboratory is currently studying the mechanism of ssDNA gap recognition by rat and human pol β.

ACKNOWLEDGMENT

We thank Gloria Drennan Davis for help in preparing the manuscript.

REFERENCES

1. Kornberg, A., and Baker, T. A. (1992) in *DNA Replication*, W. H. Freeman, New York.
2. Friedberg, E. C., Walker, G. C., and Siede, W. (1995) in *DNA Repair and Mutagenesis*, ASM Press, Washington, DC.
3. Budd, M. E., and Campbell, J. L. (1997) *Mutat. Res. 384*, 157−167.
4. Prasad, R., Singhal, R. K., Srivastava, D. K., Molina, J. T., Tomkinson, A. E., and Wilson, S. H. (1996) *J. Biol. Chem. 271*, 16000−16007.
5. Sobol, R. W., Horton, J. K., Kühn, R., Hua, G., Singhal, R. K., Prasad, R., Rajewsky, K., and Wilson, S. H. (1996) *Nature 379*, 183−186.
6. Mullen, G. P., and Wilson, S. H. (1997) *Biochemistry 36*, 4713−4717.
7. Fry, M., and Loeb, L. A. (1986) in *Animal Cell DNA Polymerases*, CRC Press, Inc., Boca Raton, FL.
8. Prasad, R., Beard, W. A., and Wilson, S. H. (1994) *J. Biol. Chem. 269*, 18096−18101.
9. Singhal, R. K., and Wilson, S. H. (1993) *J. Biol. Chem. 268*, 15906−15911.
10. Wiebauer, K., and Jiricny, J. (1990) *Proc. Natl. Acad. Sci. U.S.A. 87*, 5842−5845.
11. Matsumoto, Y., and Bogenhagen, D. F. (1989) *Mol. Cell. Biol. 9*, 3750−3757.
12. Matsumoto, Y., Kim, K., and Bogenhagen, D. F. (1994) *Mol. Cell. Biol. 14*, 6187−6197.
13. Singhal, R. K., Prasad, R., and Wilson, S. H. (1995) *J. Biol. Chem. 270*, 949−957.
14. Matsumoto, Y., Kim, K., Katz, D. S., and Feng, J.-A. (1998) *Biochemistry 37*, 6456−6464.
15. Hübscher, U., Nasheuer, H.-P., and Syväoja, J. E. (2000) *Trends Biochem. Sci. 25*, 143−147.
16. Zmudzka, B. Z., SenGupta, D., Matsukage, A., Cobianchi, F., Kumar, P., and Wilson, S. H. (1986) *Proc. Natl. Acad. Sci. U.S.A. 83*, 5106−5110.
17. Liu, D., Prasad, R., Wilson, S. H., DeRose, E. F., and Mullen G. P. (1996) *Biochemistry 35*, 6188−6200.
18. Pelletier, H., Sawaya, M. R., Kumar, A., Wilson, S. H., and Kraut, J. A. (1994) *Science 264*, 1891−1903.
19. Pelletier, H., Sawaya, M. R., Wolfle, W., Wilson, S. H., and Kraut, J. A. (1996) *Biochemistry 35*, 12762−12777.
20. Kumar, A., Abbotts, J., Karawya, E. M., and Wilson, S. H. (1990) *Biochemistry 29*, 7156−7159.
21. Casas-Finet, J. R., Kumar, A., Morris, G., Wilson, S. H., and Karpel, R. L. (1991) *J. Biol. Chem. 266*, 19618−19625.
22. Jezewska, M. J., Rajendran, S., and Bujalowski W. (1998) *J. Mol. Biol. 284*, 1113−1131.
23. Rajendran, S., Jezewska, M. J., and Bujalowski, W. (1998) *J. Biol. Chem. 273*, 31021−31031.
24. Matsumoto, Y., and Kim, K. (1995) *Science 269*, 699−702.
25. Edelhoch, H. (1967) *Biochemistry 6*, 1948−1954.
26. Bujalowski, W., Klonowska, M. M., and Jezewska, M. J. (1994) *J. Biol. Chem. 269*, 31350−31358.
27. Jezewska, M. J., and Bujalowski, W. (1996) *Biochemistry 35*, 2117−2128.
28. Jezewska, M. J., Kim, U.-S., and Bujalowski, W. (1996) *Biochemistry 35*, 2129−2145.
29. Gill, S. C., and von Hippel, P. H. (1989) *Anal. Biochem. 182*, 319−326.
30. Secrist, J. A., Bario, J. R., Leonard, N. J., and Weber, G. (1972) *Biochemistry 11*, 3499−3506.
31. Ledneva, R. K., Razjivin, A. P., Kost, A. A., and Bogdanov, A. A. (1977) *Nucleic Acids Res. 5*, 4226−4243.
32. Bujalowski, W., and Jezewska, M. J. (1995) *Biochemistry 34*, 8513−8519.
33. Bujalowski, W., and Klonowska, M. M. (1994) *Biochemistry 33*, 4682−4694.
34. Jezewska, M. J., and Bujalowski, W. (2000) *Biochemistry 39*, 10454−10467.
35. Bujalowski W., and Jezewska, M. J. (2000) in *Spectrophotometry & Spectrofluorimetry. A Practical Approach* (Gore, M. G., Ed.) Chapter 5, Oxford University Press, Oxford, U.K.
36. Jezewska, M. J., and Bujalowski, W. (1997) *Biophys. Chem. 64*, 253−269.
37. McGhee, J. D., and von Hippel, P. H. (1974) *J. Mol. Biol. 86*, 469−489.
38. Bujalowski, W., Lohman, T. M., and Anderson, C. F. (1989) *Biopolymers 28*, 1637−1643.
39. Epstein, I. R. (1978) *Biophys. Chem. 8*, 327−339.
40. Record, M. T., Lohman, T. M., and deHaseth, P. L. (1976) *J. Mol. Biol. 107*, 145−158.
41. Record, M. T., Jr., Anderson, C. F., and Lohman, T. M. (1978) *Q. Rev. Biophys. 11*, 103−178.
42. Olmsted, M. C., Anderson, C. F., and Record, M. T. (1989) *Proc. Natl. Acad. Sci. U.S.A. 86*, 7766−7770.
43. Von Hippel, P. H., and Schleich T. (1969) in *Structure of Biological Macromolecules* (Timasheff, S., and Fasman, G. D., Eds.) Chapter 6, Marcel Dekker, New York.
44. Jezewska, M. J., Rajendran, S., Bujalowska, D., and Bujalowski, W. (1998) *J. Biol. Chem. 273*, 10515−10529.
45. Baker, B. M., Vanderkooi, J., and Kallenbach, N. R. (1978) *Biopolymers 17*, 1361−1372.
46. Tolman, G. L., Barrio, J. R., and Leonard, N. J. (1974) *Biochemistry 13*, 4869−4878.
47. Doherty, A. J., Serpell, L. C., and Ponting, C. P. (1996) *Nucleic Acids Res. 24*, 2488−2497.
48. Maciejewski, M. W., Liu, D., Prasad, R., Wilson, S. H., and Mullen, G. P. (2000) *J. Mol. Biol. 296*, 229−253.
49. Saenger, W. (1984) *Principles of Nucleic Acid Structure*, Springer-Verlag, New York.

BI002749S